Allergology International. 2013;62:309-322
DOI: 10.2332/allergolint.12-OA-0528

ORIGINAL ARTICLE

The Role of Tumor Necrosis Factor-α and Interferon-γ in Regulating Angiomotin-Like Protein 1 Expression in Lung Microvascular Endothelial Cells

Yoshio Nakajima[1], Yutaka Nakamura[1], Wataru Shigeeda[2], Makoto Tomoyasu[2], Hiroyuki Deguchi[2], Tatsuo Tanita[2] and Kohei Yamauchi[1]

ABSTRACT

Background: Angiogenesis in the alveolar septa is thought be a critical factor in pulmonary emphysema. Angiomotin-like protein 1 (AmotL1) is involved in angiogenesis *via* regulating endothelial cell function. However, the role of AmotL1 in the pathogenesis of pulmonary emphysema has not been elucidated. The objective of this study is to evaluate the expression of AmotL1 in lung tissues from a murine model with emphysema, as well as from patients with chronic obstructive pulmonary disease (COPD). Furthermore, we analyzed the regulation of AmotL1 expression by TNF-α and IFN-γ in endothelial cells *in vitro*.

Methods: *Nrf2* knockout mice were exposed to cigarette smoke (CS) for 4 weeks, and the down-regulated genes affecting vascularity in the whole lung were identified by microarray analysis. This analysis revealed that the mRNA expression of AmotL1 decreased in response to CS when compared with air exposure. To confirm the protein levels that were indicated in the microarray data, we determined the expression of AmotL1 in lung tissues obtained from patients with COPD and also determined the expression of AmotL1, NFκB and IκBα in cultured normal human lung microvascular endothelial cells (HLMVECs) that were stimulated by TNF-α and IFN-γ.

Results: We found that the number of AmotL1-positive vessels decreased in the emphysema lungs compared with the normal and bronchial asthmatic lungs. IFN-γ pretreatment diminished the TNF-α-induced AmotL1 in the cultured HLMVECs by blocking the degradation of IκBα.

Conclusions: These results suggested that IFN-γ exhibits anti-angiogenesis effects by regulating the expression of TNF-α-induced AmotL1 *via* NFκB in emphysema lungs.

KEY WORDS

angiogenesis, angiomotin, angiomotin-like protein 1, COPD, emphysema

INTRODUCTION

Chronic obstructive pulmonary disease (COPD), which is primarily a smoking-related inflammatory lung disease, can be defined by chronic airflow limitation confirmed by spirometry.[1] Tumor necrosis factor (TNF)-α and interferon (IFN)-γ levels are significantly elevated compared with healthy smokers and non-smokers, and these cytokines are apparently involved in the pathogenesis of COPD as primary mediators that drive the inflammation that is characteristic of COPD.[2-4] Angiogenesis has also been suggested to be one of the critical factors in the pathogenesis of pulmonary emphysema. Based on the ob-

[1]Division of Pulmonary Medicine, Allergy, and Rheumatology, Department of Internal Medicine and [2]Department of Thoracic Surgery, Iwate Medical University School of Medicine, Iwate, Japan.
Conflict of interest: No potential conflict of interest was disclosed.
Correspondence: Yutaka Nakamura, Division of Pulmonary Medicine, Allergy, and Rheumatology, Department of Internal Medicine, Iwate Medical University School of Medicine, 19–1 Uchimaru, Morioka, Iwate 020–8505, Japan.
Email: ICB75097@nifty.com
Received 11 December 2012. Accepted for publication 19 February 2013.

servation that the alveolar septa in centrilobular emphysema are remarkably thin and avascular, Liebow theorized that a reduced blood supply from small precapillary blood vessels might induce the disappearance of the alveolar septa.[5] This hypothesis for the pathogenesis of emphysema has been supported by the results of a recent study in which the expression of both vascular endothelial growth factor (VEGF) and its receptors were decreased in the lung tissues of emphysema patients.[6,7] However, the effects of TNF-α and IFN-γ on angiogenesis in emphysema have not been fully elucidated. We hypothesize that increased levels of TNF-α and IFN-γ will interact in lung endothelial cells and result in hypovascularity. In the present study, we demonstrated that the mRNA and protein expression levels of angiomotin-like protein 1 (AmotL1) in whole lungs were decreased in cigarette smoke (CS)-exposed *NF-E2 related factor 2* (*Nrf2*) knockout (*Nrf2*$^{-/-}$) mice compared with those in the *Nrf2*$^{-/-}$ mice without CS exposure. AmotL1 is involved in angiogenesis *via* the regulation of endothelial cell function. Amot, together with AmotL1 and AmotL2, belongs to a novel protein family that is characterized by a conserved glutamine-rich domain.[8,9] AmotL1 was initially cloned from a mouse pancreatic islet endothelial cell line as a tight junction-enriched and associated protein.[10,11] The biological function of AmotL1 has been reported to regulate sprouting angiogenesis by influencing tip cell migration and controlling the cell-cell junctions of stalk cells.[12] We also identified the promoter segment for the *AmotL1* gene in normal human lung microvascular endothelial cells (HLMVECs) as the -387 to -372 region upstream from the translation initiation codon. NFκB was found to bind to this *AmotL1* promoter region. *In vitro* investigations using HLMVECs have revealed that TNF-α induced AmotL1 expression *via* NFκB, whereas TNF-α-induced IκBα degradation is completely suppressed in HLMVECs by IFN-γ treatment. These studies demonstrate the role of a novel angiogenic molecule, AmotL1, which is regulated by TNF-α and IFN-γ, in pulmonary emphysema.

METHODS

ANIMAL CARE AND CIGARETTE SMOKE EXPOSURE

All of the animal protocols used in this study were approved by the National Institute of Environment Health Sciences' Animal Care and Use Committee and followed the Helsinki Convention standards for the use and care of animals. The experimental procedures were approved by the institutional animal care and use committees at Iwate Medical University in accordance with the university's animal experiments regulations. The *Nrf2*$^{-/-}$ mice, which were backcrossed >20 times into a C57BL/6J background, were purchased from RIKEN BioResource Center (Ibaraki, Japan). The mice were genotyped for *Nrf2* status by the polymerase chain reaction (PCR) amplification of genomic DNA, which had been extracted from the blood as previously described.[13] All of the mice used in this study were aged 9-10 -weeks and were maintained under specific pathogen-free conditions. The mice were divided into 2 groups (n = 11 per group): control *Nrf2*$^{-/-}$ mice and experimental *Nrf2*$^{-/-}$ mice. The control groups were kept in a filtered air environment, and the CS-exposed groups were subjected to CS exposure, which was performed (5 hours per day, 5 days/week for up to 4 weeks) by burning 3R4F cigarettes (purchased from the Tobacco Research Institute, University of Kentucky, KY, USA) using a smoking apparatus (SIC-CS type, SG-200, Shibata Kagaku, Saitama, Japan). Each smoldering cigarette was puffed for 2 seconds at 5 puffs (175 ml)/min, with a flow rate of 5375.5 ml/min diluted with compressed air (3% final concentration), and then air flow (1700 ml/min) dispersed the cigarette smoke into the sealed mouse container (3600 cm^3).

LUNG HISTOLOGY AND QUANTIFICATION OF EMPHYSEMA IN THE EXPERIMENTAL MOUSE MODEL

The tracheas and lungs of the anesthetized mice were terminally removed and inflated with 4% paraformaldehyde in PBS to a pressure of 12 cm H_2O. The tissues were then embedded in paraffin, and 5-μm-thick sections were stained with hematoxylin and eosin (HE). Air space enlargement was quantified with the mean linear intercept in randomly selected fields of tissue sections. The mean linear intercept, as a measure of interalveolar septal wall distance, was measured using light microscopy at a magnification of 100×. The mean linear intercept was obtained by dividing the length of a line drawn across the lung section by the total number of intercepts encountered in 36 lines per mouse lung, as described previously.[14,15]

COLLECTION AND ANALYSIS OF BRONCHOALVEOLAR LAVAGE FLUID OF THE EXPERIMENTAL MICE

Bronchoalveolar lavage (BAL) was performed as described previously.[16] All BAL fluid (1 ml of saline solution 2 separate times) was collected, and BAL cells were counted. Cell types were identified based on morphological criteria. The absolute numbers of each cell type were calculated. One hundred thousand viable BAL cells were cytocentrifuged onto slides and stained with May-Grünwald-Giemsa solution. CD8+ cells were detected using immunocytochemistry (R& D Systems, MN, USA). To determine cytokine concentrations, we centrifuged samples at 1,200 rpm for 5 min at 4℃. Supernatants were analyzed by specific ELISA to determine the concentrations of TNF-α, IFN-γ (BD, NJ, USA), AmotL1 (Cusabio Biotech, Hubei, China), and VEGF (RayBiotech, GA, USA),

and with commercially available kits.

MICROARRAY ANALYSIS

The expression of RNA from the whole lungs that were obtained from the CS-exposed or non-exposed mice was assessed as described previously.[17] The microarray analysis revealed that the mRNA expression of AmotL1, which is relevant to angiogenesis, decreased in response to CS compared with no exposure to CS.

IMMUNOHISTOCHEMISTRY

Immunolocalization of AmotL1 in the lung tissue was evaluated using polyclonal anti-AmotL1 (Assay Biotechnology, CA, USA). AmotL1 was detected by diaminobenzidine, and the sections were counterstained with hematoxylin. Negative control experiments were conducted by replacing the primary antibody with an isotype-matched control. All of the cells from the individual lung specimens were analyzed using an Olympus DP 70 system (Olympus, Tokyo, Japan). The results are expressed as the mean number of AmotL1-positive vessels in 5 randomly selected fields of tissue sections ± SE per mouse lung. We then examined the correlation between the mean linear intercept and the AmotL1-stained vessels in the tissue sections derived from the CS-exposed mice (n = 11).

SUBJECTS

This study was also approved by the Iwate Medical University Hospital Ethics Committee. Informed consent was obtained from the subjects. Lung tissue samples from ex-smoker controls (control, n = 5), ex-smokers with bronchial asthma (n = 5), and moderate COPD (GOLD 2) patients (n = 5) were obtained by surgical resection for lung cancer. The control and asthmatic subjects were matched by age to the COPD subjects. All of the subjects had >20 pack-year histories. The bronchial asthma and COPD subjects were selected using the American Thoracic Society criteria, and these individuals used an inhaled β-agonist on demand, as well as an inhaled long-acting β2-agonist (LABA) and inhaled corticosteroids (ICS) twice per day. None of the patients had previously used any other anti-inflammatory drugs, such as leukotriene modifiers, or sodium cromoglicate within the previous 3 months. Furthermore, these patients had no other medical disorders. Five-micrometer tissue sections were affixed to microscope slides and prepared for analysis. Immunolocalization of AmotL1 in the lung tissue was performed using polyclonal anti-AmotL1 (Assay Biotechnology). The individual results were expressed as the mean number of AmotL1-positive vessels in 20 randomly selected fields of tissue sections ± SE.

IMMUNOBLOT ANALYSIS OF AmotL1 IN HUMAN LUNG MICROVASCULAR ENDOTHELIAL CELLS

Normal human lung microvascular endothelial cells (HLMVECs) were purchased from Takara (Tokyo, Japan) and maintained in an EGM-2-MV BulletKit (Takara) according to the manufacturer's instructions. The HLMVECs that were treated with or without 100 ng/mL TNF-α (R&D Systems) or IFN-γ (R&D Systems) were collected and lysed in TNE buffer, as previously described.[18] Twenty micrograms of protein was resolved by 10% SDS-PAGE and transferred to a polyvinylidene difluoride membrane (Bio-Rad, CA, USA). The membrane was incubated with a rabbit polyclonal anti-human AmotL1 (Sigma-Aldrich, MO, USA) or a GAPDH (R&D Systems) antibody, which was detected using an infrared detection method (LI-COR, NE, USA) according to the manufacturer's instructions. The membranes were analyzed using the Odyssey Infrared Imaging System (LI-COR), and where relevant, the signal intensity was determined using LI-COR imaging software and exported to JMP version 8.0.2 (SAS Institute Japan, Tokyo, Japan) for graphical representation as the mean ± SE.

PREPARATION OF CELL LYSATES AND PROBES FOR THE ELECTROPHORETIC MOBILITY SHIFT ASSAY (EMSA)

Because the putative AmotL1 promoter in HLMVECs has not been identified, we searched for binding sites within the AmotL1 promoter region using the UCSC Genome Browser and TRANSFAC database.[19] This approach revealed NFκB elements that were regulated by TNF-α in the AmotL1 promoter region. HLMVECs that were pretreated with or without TGF-β (negative control) or IFN-γ were stimulated with 100 ng/mL TNF-α for 0.5 h. Nuclear extracts were prepared from the HLMVECs as previously described.[18] A protein assay (Bio-Rad) was performed to determine the nuclear protein concentration. Complimentary oligonucleotides (5'-AGTGGAATTTCCAG GTAGA-3' and 5'-CCTGGAAATTCCACTTAAG-3') containing NFκB binding sites in the human AmotL1 promoter region with four-base overhangs were combined, boiled in 0.5 M NaCl, and cooled to room temperature. Mutated NFκB -binding sites (5'-AGTGTGT ATACCAGGTAGA-3' and 5'-CCTGGTATACACACTT AAG-3') were used as a negative control. Note that the underlining identifies the mutated sequences. The oligonucleotides were end-labeled with an infrared fluorophore (Metabion International, Martinsried, Germany). Probe oligonucleotides containing GATA-1-binding sites (5'-ACTCAGGCAGATAAC AG -3' and 5'-CAGGCTGTTATCTGCCT -3'), mutated GATA-1-binding sites (5'-ACTCACAGGTAGACAAG-3' and 5'-CAGGCTTGTCTACCTGT -3'), containing Stat-5- binding sites (5'-TTATGGCCAGAAG GATG T ACGGTTCTGCG AAC-3' and 5'-ATGTGTTCG CAGA

ACCGTACATCCTCTGGCC-3'), and mutated Stat-5-binding sites (5'-TTATGCAGCAGAGTGGACGTACT TGAA CGTGC-3' and 5'-ATGTGCACGTTCAAGTAC GTCCACTCTGCTGC-3') were also used. Ten micrograms of the nuclear extracts and IRD700-labeled double-strand oligomers were incubated in binding buffer (20% glycerol, 20 mM HEPES, 100 mM KCl, 20 mM Tris-HCl, 1 mM EDTA, and 1 mM DTT), with or without unlabeled competitors, for 30 min at room temperature. After a 30-min pre-run of the gel, the samples were loaded onto 7.5% native polyacrylamide gels in 0.25× Tris-borate-EDTA buffer and run at 120 V for 3 h at 4℃. The gels were visualized under infrared light. The membranes were analyzed using the Odyssey Infrared Imaging System (LI-COR), and where relevant, the signal intensity was determined using LI-COR imaging software and exported to JMP version 8.0.2 (SAS Institute Japan) for graphical representation as the mean ± SE.

KNOCKDOWN OF p65 AND AmotL1 EXPRESSION USING SHORT HAIRPIN RNA

Short hairpin (sh) RNA oligonucleotides for the NFκB p65 plasmid was purchased from Santa Cruz Biotechnology (CA, USA). The plasmid was a target-specific lentiviral vector engineered for knockdown gene expression. For the shRNA delivery, 2×10^5 HLMVECs were plated in 6-well plates 2 days prior to the transfection. The cells were transfected with shRNA Plasmid Transfection Regent (Santa Cruz Biotechnology), following the manufacturer's instructions, and were then stimulated with TNF-α at 24 h post-transfection. The control plasmid was a transfection-ready lentiviral vector that encoded GFP in mammalian cells and was employed to monitor the delivery of the shRNA lentiviral construct into the cells, thereby gauging the transfection efficiency. The maximum transfection efficiency was observed at 16 h post-transfection.

IκBα EXPRESSION IN CYTOPLASMIC EXTRACTS

To determine the effect of the IFN-γ on IκBα expression, cytoplasmic extracts were prepared from 2×10^6 HLMVECs/ml treated with 100 ng/mL IFN-γ for 72 h and then treated with 100 ng/mL TNF-α for different time periods. Cytoplasmic extracts were prepared from cultured HLMVECs as described previously.[18] The extracts were resolved with 10% SDS-PAGE and analyzed with immunoblotting using antibodies against IκBα (R&D Systems). After electrophoresis, the proteins were detected by an infrared detection method (LI-COR, NE, USA) according to the manufacturer's instructions.

STATISTICAL ANALYSIS

All of the data are expressed as the mean ± SE. The number of cells in the BAL and the AmotL1- positive vessels in lung tissues from air-exposed mice and CS-exposed mice were compared using the unpaired Student's *t* test. The correlation between the linear intercept and the number of AmotL1-positive vessels was performed using correlation analysis. One-way ANOVA was used to assess the differences among three or four groups. JMP version 8.0.2 software (SAS Institute Japan) was used for the statistical analyses. Differences with p values < 0.05 were considered statistically significant.

RESULTS

DEVELOPMENT OF EMPHYSEMA IN *Nrf2*$^{-/-}$ MOUSE LUNGS AS DETERMINED IN HISTOLOGICAL AND INFLAMMATORY CELL STUDIES

We first evaluated the development of emphysema in *Nrf2*$^{-/-}$ mice after up to 4 weeks of CS exposure using HE-stained lung sections. No pathological findings were observed in the *Nrf2*$^{-/-}$ mice before or after 4 weeks of air exposure (Fig. 1a-c). In the *Nrf2*$^{-/-}$ mice, airspace enlargement and alveolar wall obstruction were both observed 4 weeks after the initial CS exposure (Fig. 1d). To further characterize the development of emphysema in the *Nrf2*$^{-/-}$ mice, we determined the degree of airspace enlargement by measuring the mean linear intercept in 36 randomly selected fields. The mean linear intercept values in the *Nrf2*$^{-/-}$ mice were approximately 3-times higher than the values found in the control *Nrf2*$^{-/-}$ mice 4 weeks after treatment ($p < 0.01$) (Fig. 1e). This histological evaluation demonstrated that the *Nrf2*$^{-/-}$ mice developed emphysema. Exposure to CS increased the absolute numbers of total cells (Fig. 1f), alveolar macrophages (Fig. 1g), neutrophils (Fig. 1h), and CD 8-positive T lymphocytes (Fig. 1i) in the BAL fluid of mice, compared with air-exposed mice ($p < 0.01$).

EFFECTS OF CS EXPOSURE ON THE VASCULAR GENE EXPRESSION PROFILES OF *Nrf2*$^{-/-}$ MICE, AS MEASURED BY cDNA MICROARRAY AND IMMUNOHISTOCHEMISTRY

The tissue hypovascularity that was observed in the emphysema patients suggested that the vasculature strongly responded to the CS, resulting in emphysema. To test this idea, we compared the mRNA expression between the CS-exposed and control *Nrf2*$^{-/-}$ mice by microarray analysis. The AmotL1 mRNA expression in the lung decreased in response to the CS-exposure compared with the control *Nrf2*$^{-/-}$ mice (Table 1). AmotL1 mRNA expression was decreased in the lungs of the CS-exposed *Nrf2*$^{-/-}$ mice to a value that was 10% below that of the air-exposed *Nrf2*$^{-/-}$ mice. We next confirmed the protein levels of AmotL1 in the BAL fluid recovered from the mice. We also measured the concentration of another angiogenic factor, VEGF, and proinflammatory cytokines that are implicated in emphysema, specifically TNF-α and IFN-γ, in BAL fluid. As expected in this model,

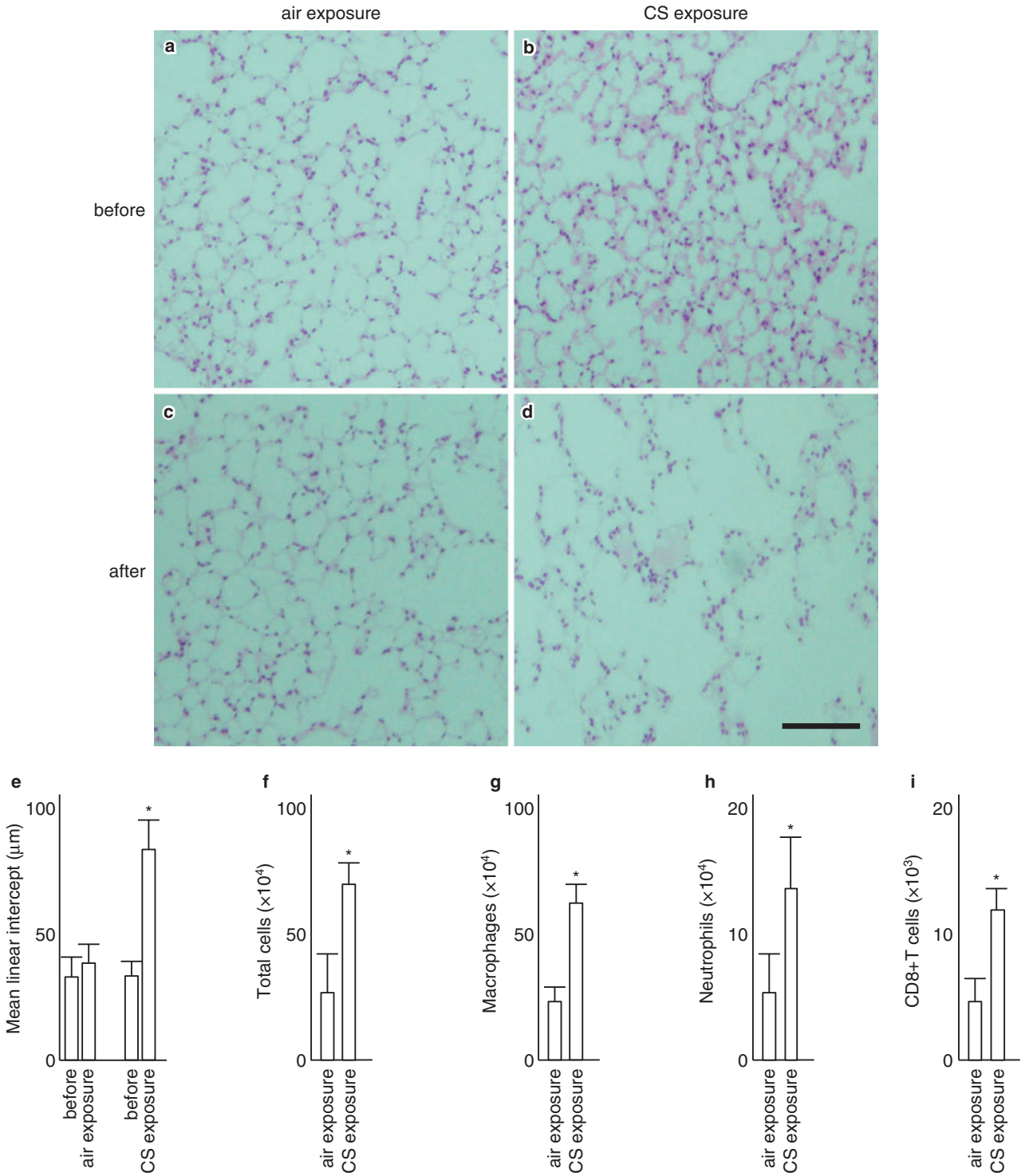

Fig. 1 Cigarette smoke (CS) exposure induced emphysema and increased bronchoalveolar lavage (BAL) cells in the mice. Shown are the hematoxylin and eosin stains of lung tissue sections (40×) from the *Nrf2*$^{-/-}$ mice before either **a**) air or **b**) CS exposure and 4 weeks after **c**) air or **d**) CS exposure. Sections from the air-exposed *Nrf2*$^{-/-}$ mice exhibited normal alveolar structure (n = 11 per group). Lung sections from the CS-exposed *Nrf2*$^{-/-}$ mice exhibited increased air space enlargement compared with the lung sections from the air-exposed *Nrf2*$^{-/-}$ mice. Scale bar: 100 μm. **e**) The mean values of the linear intercept in the cigarette smoke-exposed *Nrf2*$^{-/-}$ mice were significantly greater than those values from the air-exposed *Nrf2*$^{-/-}$ mice. The values are expressed as the means ± SE from 36 images per lung section. **f**) Total cell counts, **g**) macrophages, and **h**) neutrophils were calculated on cytospin slides. **i**) CD8+ T cells were enumerated by immunocytochemical analysis. *indicates $p < 0.01$ vs. the air-exposed mice.

Table 1 Summary of cigarette smoke-induced emphysema associated genes identified by microarray analyses

Gene name	Gene accession number	Expression ratio
Clca3	NM_017474	0.0495
AmotL1	NM_001081395	0.0744
B4galnt4	NM_177897	0.137
Srcrb4d	NM_001160366	0.1483
Slc16a4	NM_146136	0.1558
Olfr782	NM_001011797	0.1655
Celsr3	NM_080437	0.1678
Clec12b	NM_027709	0.1780
Nr1d1	NM_145434	0.1805
Cpne5	NM_153166	0.1829
Col24a1	NM_027770	0.190
Ppbp	NM_023785	0.1908
Ccl24	NM_019577	0.2106
CD209a	NM_133238	0.2187
Gp9	NM_018762	0.2212
Gm129	NM_001033302	0.2256

the BAL fluid concentrations of AmotL1 (Fig. 2a) and VEGF (Fig. 2b) were markedly decreased in CS-exposed mice compared to air-exposed mice. The levels of the proinflammatory cytokines, TNF-α and IFN-γ, in the BAL fluid from CS-exposed mice were significantly higher than those from air-exposed mice (not shown). To clarify which cell types express AmotL1, the lungs were immunostained with anti-AmotL1 antibody. In the control mice, the endothelial cells were strongly stained with AmotL1 4 weeks after air exposure (Fig. 2c). In contrast, only a few cells that were positively stained with the AmotL1 antibody were observed in the lungs of the *Nrf2*$^{-/-}$ mice that were exposed to CS (Fig. 2d). Compared with lung specimens from air-exposed mice, the number of vessels expressing AmotL1 protein was significantly decreased in specimens from CS-exposed mice ($p < 0.05$) (Fig. 2e). We examined the relationship between the linear intercept and the number of AmotL1-positive vessels in CS-exposed mice. The linear intercept was inversely correlated with AmotL1 expression in the lung vessels ($r = -0.77$; $p < 0.01$) (Fig. 2f).

IMMUNOHISTOCHEMISTRY OF AmotL1 EXPRESSION IN THE LUNGS OF PATIENTS

AmotL1 expression was examined in the lungs obtained from the control, bronchial asthmatic, and emphysema subjects. The AmotL1-positive cells were localized to the endothelial cells and alveolar macrophages. As shown in Figure 3a-c, AmotL1-positive cells were detected in all of the patient groups. The AmotL1 protein levels of the vessels were significantly lower in the emphysema patients compared with the control and asthmatic patients ($p < 0.05$) (Fig. 3d).

IFN-γ SUPPRESSES TNF-α-INDUCED AmotL1 EXPRESSION

HLMVECs were treated with 100 ng/ml IFN-γ for 72 h and then stimulated with TNF-α for 24 h, 48 h, and 72 h and examined for AmotL1 expression by immunoblotting. As shown in Figure 4, TNF-α induced a 3-fold increase in AmotL1, and the IFN-γ pretreatment diminished the TNF-α-induced AmotL1 expression. IFN-γ alone did not induce AmotL1 protein expression in the HLMVECs.

TNF-α INCREASES NFκB BINDING ACTIVITY AT THE AmotL1 PROMOTER REGION

EMSA was performed to examine the AmotL1-binding activity in the HLMVECs that were treated with TNF-α for 0.5 h (Fig. 5a, b). Nuclear extract induction from the HLMVECs with double-strand oligonucleotides contained the NFκB binding site but not the GATA-1 or Stat-5 binding sites (data not shown) in the human AmotL1 promoter regions that yielded mobility-shifted complexes. An excess of unlabeled specific competitor abolished binding to the labeled oligonucleotides and NFκB complexes, whereas 10- and 20-fold molar excesses of the mutant competitor oligonucleotide had no effect on the NFκB binding activity. These data suggest that NFκB might contribute to AmotL1 up-regulation in HLMVECs exposed to TNF-α.

IFN-γ INHIBITS TNF-α-INDUCED NFκB ACTIVATION

IFN-γ also potentially helps to regulate emphysema pathophysiology and immunomodulation. HLMVECs were treated with 100 ng/ml IFN-γ for 72 h and then treated with 100 ng/ml TNF-α for 0.5 h and examined for NFκB activation by EMSA. TNF-α activated NFκB, and IFN-γ pretreatment abolished the TNF-α-induced NFκB activation in a time- and dose-dependent manner (Fig. 6a and data not shown). The maximum suppression of NFκB activation was observed when the cells were treated with 100 ng/ml IFN-γ for 72 h; however, IFN-γ alone did not activate NFκB (data not shown). In addition to TNF-α, NFκB is also activated by a wide variety of other agents, including IL-1, LPS, and TGF-β. The results indicated that TGF-β did not affect the NFκB activation that was induced by TNF-α (Fig. 6a, b).

TRANSFECTION OF HLMVECs WITH shRNA SPECIFIC FOR NFκB p65

To further investigate the role of NFκB in the expression of AmotL1, HLMVECs were transfected with either shRNA for NFκB p65 or control shRNA. To determine the transfection efficiencies, the control plasmid was also transfected with the lentiviral vector plasmid that encodes GFP. Homogenous staining of the cytoplasm and pronounced accumulation was

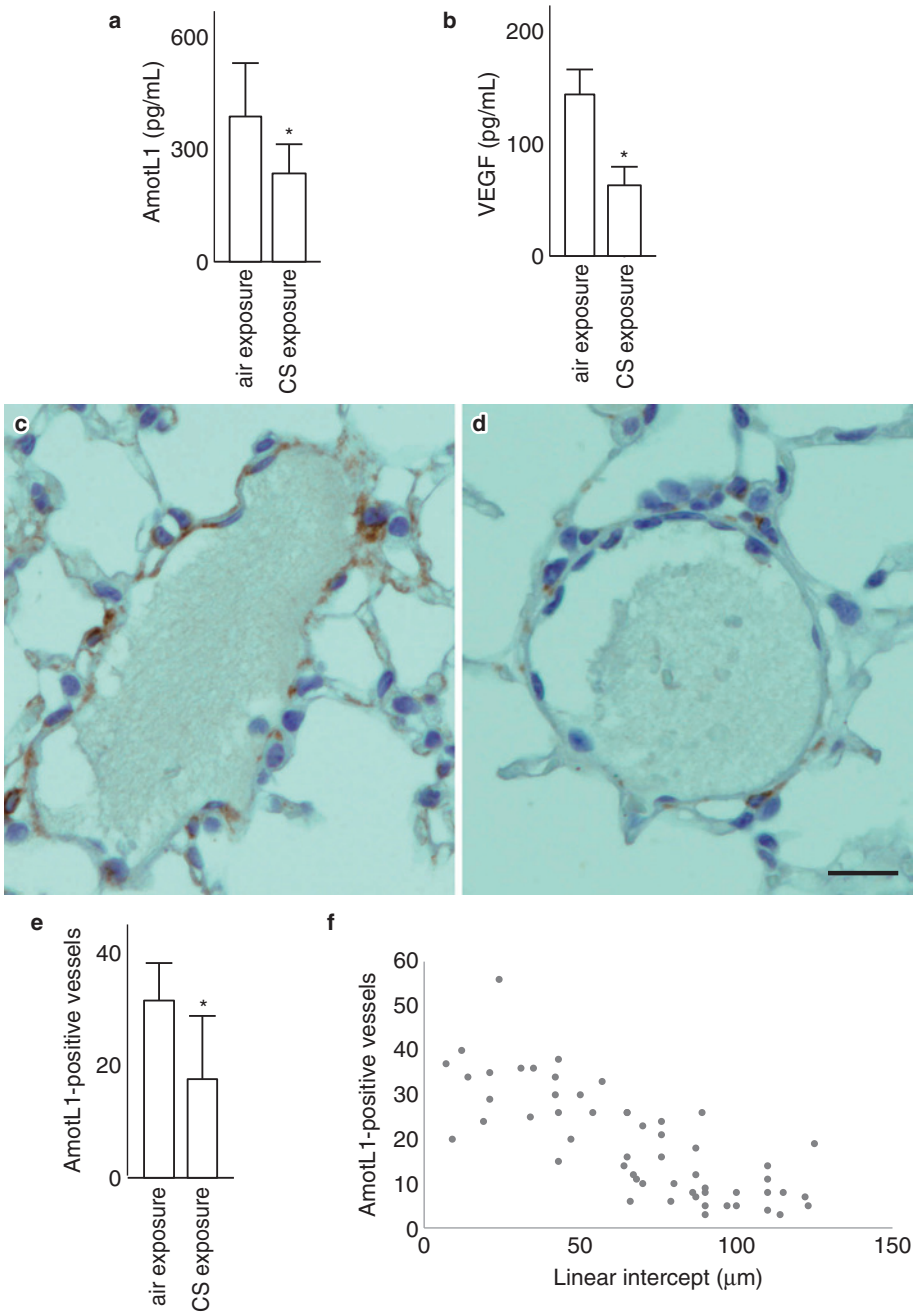

Fig. 2 Cigarette smoke (CS) exposure suppresses AmotL1 and vascular endothelial growth factor (VEGF) production in the airways of mice. Bronchoalveolar lavage (BAL) fluids of the mice were submitted to analysis for the expression of the indicated molecules. Concentrations of **a**) AmotL1 and **b**) VEGF in BAL fluid were decreased when exposed to CS. Representative photomicrographs show lung tissues stained with the AmotL1 antibody. **c**) Lung sections from the air-exposed *Nrf2*$^{-/-}$ mice. **d**) Lung sections from the CS-exposed *Nrf2*$^{-/-}$ mice. (400×) Scale bar: 20 μm. **e**) The number of AmotL1-positive vessels in the lung tissue specimens from air-exposed mice and CS-exposed mice. The values are means ± SE from 5 randomly selected fields of tissue sections per mouse lung (11 air-exposed mice and 11 CS-exposed mice). *indicates $p < 0.05$ vs. the air-exposed mice. **f**) Correlation with linear intercept of AmotL1-positive vessels in the lungs from the CS-exposed mice. The values were obtained from 5 randomly selected fields of tissue sections per mouse lung (eleven CS-exposed mice). The simple correlation coefficient (r) was -0.77, $p < 0.01$.

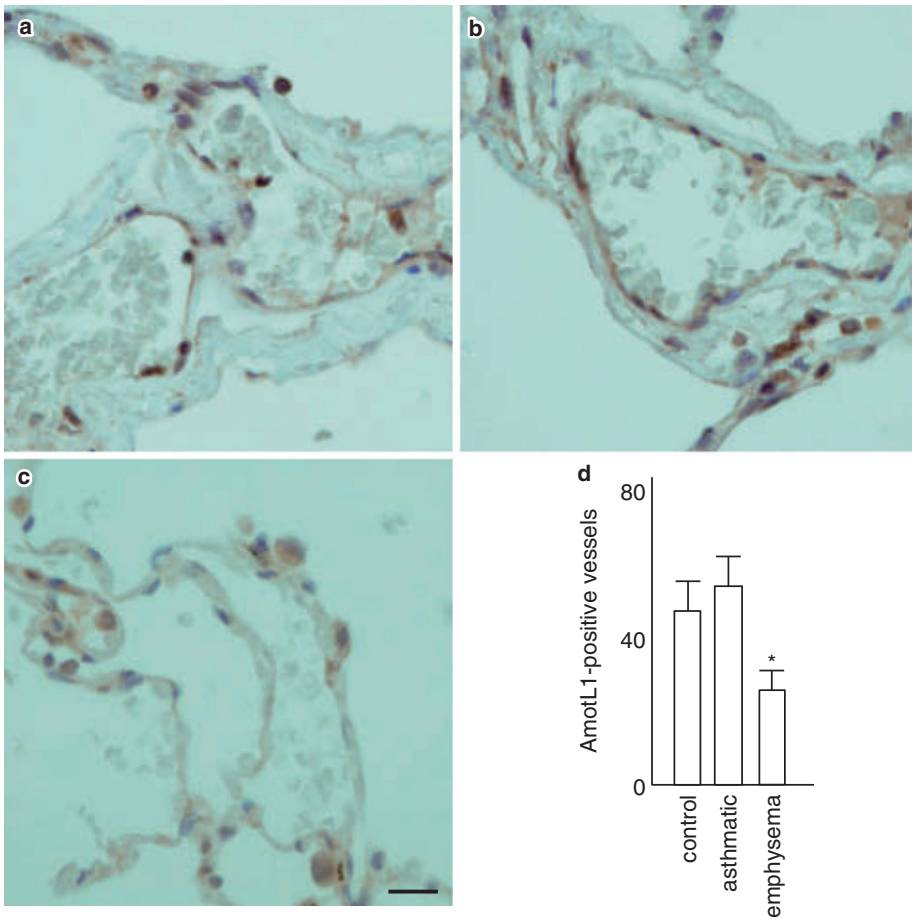

Fig. 3 Lung tissues obtained from the ex-smoker control subjects, asthmatic patients, and emphysema patients. Representative photomicrographs show lung specimens stained with an anti-AmotL1 antibody. Localization of AmotL1 with endothelial cells and macrophages was observed in the lungs from the **a**) control and **b**) asthmatic patients. **c**) Localization of AmotL1 with endothelial cells was not observed in the lungs of the emphysema patients. (400×) Scale bar: 20 μm. **d**) The number of AmotL1-positive vessels in the lung tissue specimens from the control, asthmatic, and emphysema patients. The values are means ± SE from 20 images per lung section. *indicates $p < 0.05$ vs. the control and asthmatic patients.

noted after 16 h in -90% of the HLMVECs (Fig. 7a).

NFκB CONTROLS AmotL1 EXPRESSION IN THE HLMVECs

We examined the potential of an NFκB blockade to prevent TNF-α-induced AmotL1 protein expression in HLMVECs. Adding TNF-α to the HLMVECs for 24 h significantly increased the AmotL1 activity compared with the untreated HLMVECs. To determine whether this effect was mediated by NFκB, the HLMVECs were transfected with an shRNA specific for NFκB. In the presence of the NFκB shRNA, the TNF-α-induced AmotL1 expression was reduced to baseline levels, whereas the control shRNA did not decrease the AmotL1 expression. Therefore, NFκB is required for TNF-α-induced AmotL1 regulation (Fig. 7b, c).

IFN-γ INHIBITS THE TNF-α-DEPENDENT DEGRADATION OF IκBα

To determine whether the TNF-α-induced NFκB activation was inhibited by inhibiting IκBα degradation, the HLMVECs were pretreated with 100 ng/mL IFN-γ for 72 h, exposed to 100 ng/ml TNF-α for different time periods, and then examined for IκBα expression in the cytoplasm by immunoblotting. As shown in Figure 8a, b, the TNF-α-induced IκBα degradation in the HLMVECs reached its maximum at 60 min, whereas the TNF-α-induced IκBα degradation was completely suppressed in the IFN-γ-treated cells (Fig. 8c, d).

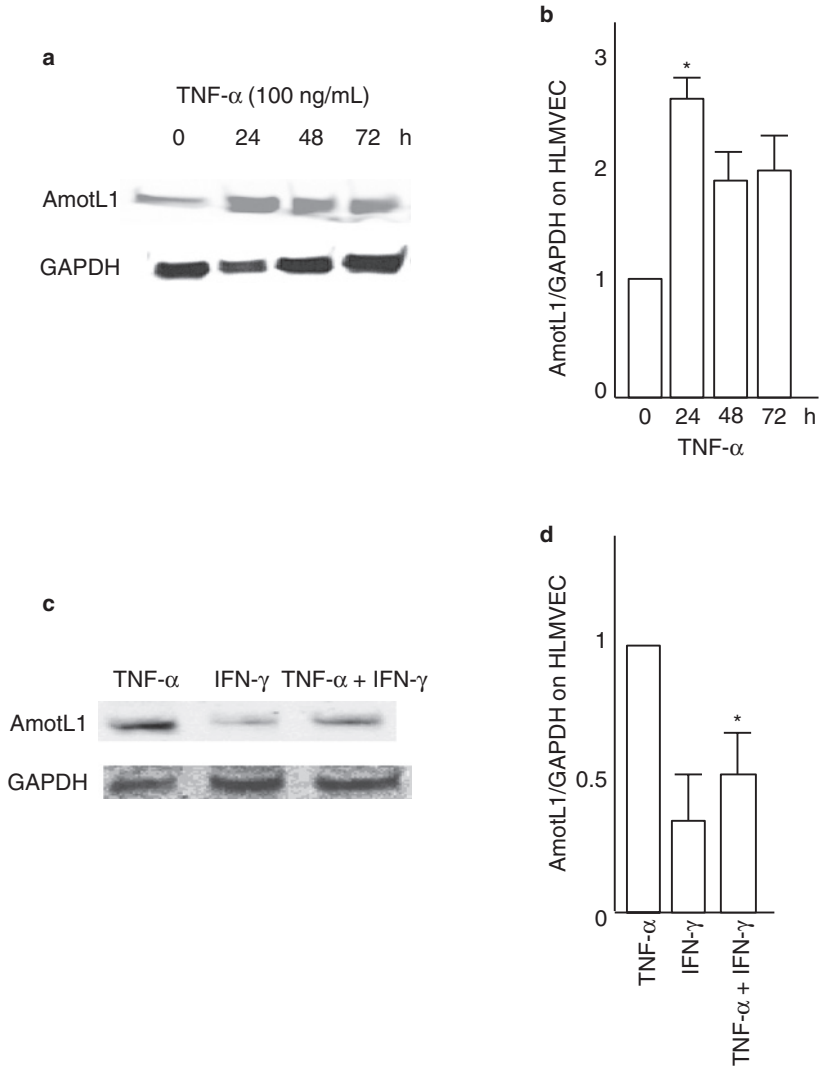

Fig. 4 Effects of IFN-γ on TNF-α-induced AmotL1 protein expression in human lung microvascular endothelial cells (HLMVECs). Stimulation with TNF-α at a concentration of 100 ng/ml for 24 h increased the AmotL1 protein expression in HLMVECs. **a**) Data are representative of five separate experiments. **b**) Summary of the data (mean ± SE) from five independent experiments. *indicates $p < 0.05$ vs. TNF-α stimulation for 0 h. HLMVECs were treated with 100 ng/ml of IFN-γ for 72 h and then stimulated with TNF-α for 24 h. The cells were then examined for AmotL1 expression by immunoblotting. IFN-γ pretreatment diminished the TNF-α-induced AmotL1 expression. IFN-γ alone did not induce AmotL1 protein expression in the HLMVECs. **c**) Data are representative of five separate experiments. **d**) Summary of the data (mean ± SE) of five independent experiments. *indicates $p < 0.05$ vs. the TNF-α stimulation condition.

DISCUSSION

Several new findings have emanated from this study. First, we demonstrated that AmotL1 expression was significantly decreased in the lungs of the CS-exposed mice compared with the control mice. The AmotL1-positive cells were phenotypically identified as endothelial cells and macrophages. Second, we found that the number of AmotL1-positive blood vessels was decreased in the emphysema patients compared with the control and asthmatic patients. Third, we determined that TNF-α increased AmotL1 expression in HLMVECs *via* the transcription factor NFκB. Finally, IFN-γ suppressed TNF-α-dependent IκBα degradation in the HLMVECs.

We elected to forgo the use of the most common

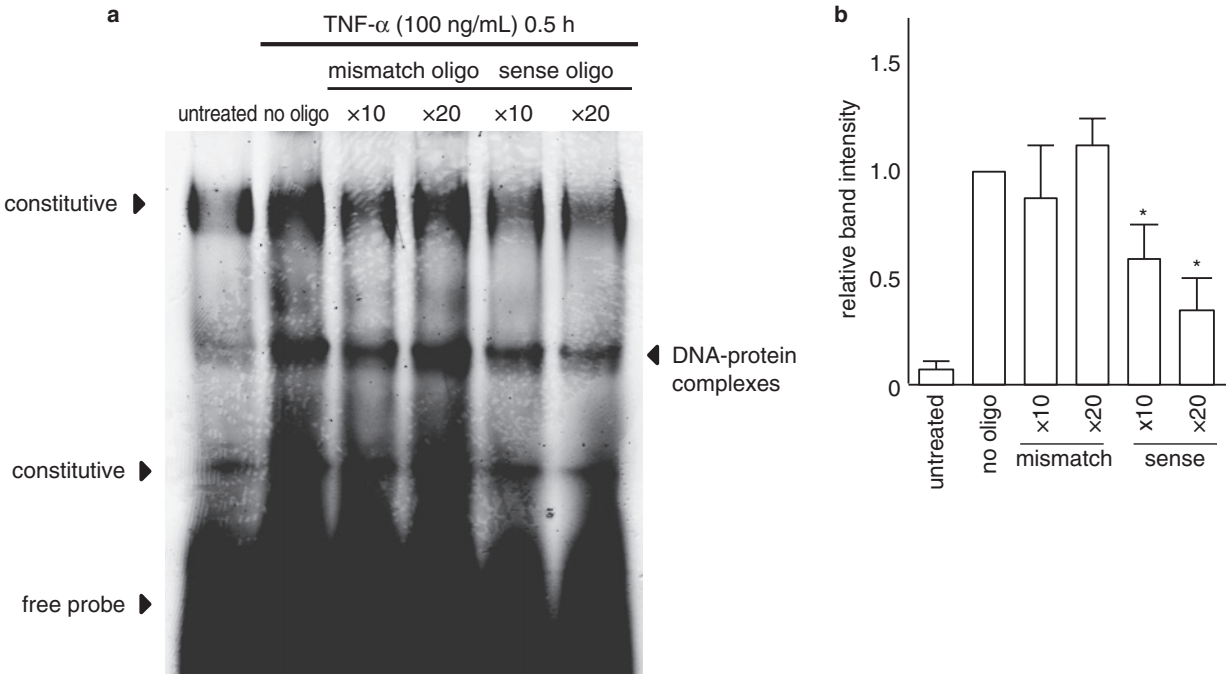

Fig. 5 Electrophoretic mobility shift assay (EMSA) for AmotL1-binding activity. EMSA with nuclear extracts from human lung microvascular endothelial cells (HLMVECs) treated with or without TNF-α at 100 ng/ml for 0.5 h and incubated with an infrared fluorophore, which shows double-stranded oligonucleotides containing the NFκB-binding site in the AmotL1 promoter region. **a**) Competition assays with unlabeled homologues or mismatch oligonucleotides. *lane 1*, without TNF-α stimulation; *lane 2*, no competitor; *lane 3* and *lane 4*, excess mismatch competitor (*lane 2*, 10-fold excess; *lane 3*, 20-fold excess); *lane 5* and *lane 6*, excess unlabeled specific competitor (*lane 5*, 10-fold excess; *lane 6*, 20-fold excess). **b**) Quantification of the EMSA with the infrared fluorophore-labeled AmotL1 promoter region. Summary of the data (mean ± SE) of five independent experiments. *indicates $p < 0.05$ vs. the no oligo condition.

CS-induced emphysema model, using C57BL/6 J mice, preferring to use *Nrf2*$^{-/-}$ mice, which were backcrossed into a C57BL/6J background. This choice was based on compelling data that led us to believe that this approach would be better. However, of particular concern with the *Nrf2*$^{+/+}$ mouse is that the need for more than 6 months of CS exposures often results in complicating age-associated vessel structure phenotypes. Singh *et al*. have demonstrated an emphysema model using 4-weeks-CS-exposed *Nrf2*$^{-/-}$ mice.[20] Although we did not assess or report on the lung mechanics, such as the static lung compliances, it was demonstrated that the BAL cells and histological findings from 4-weeks-CS-exposed *Nrf2*$^{-/-}$ mice were in agreement with previous emphysema mouse models. In our preliminary studies, we could not demonstrate that there was a significant increase of BAL cells and airspace enlargement with variable components of angiogenic factors in the 4-weeks-CS-exposed *Nrf2*$^{+/+}$ mice. Then, we verified the expression of molecules that the mouse model indicated might be expressed in the tissues from controls and patients with COPD.

There are several candidate angiogenic factors with pathogenic roles in emphysema, the most frequent of which is VEGF. Normal lung function and the ability of the lung to respond to damage appear to be critically dependent on the presence of locally functioning VEGF.[6,7] VEGF deficiency augments oxidant injury and tissue destruction and has been implicated in the pathogenesis of pulmonary emphysema and other disorders. However, the processes that regulate VEGF tissue responses in the lung have not been elucidated. Recently, Elias and colleagues have demonstrated that influenza and respiratory syncytial virus exert similar inhibitory effects on vascular remodeling *via* the IFN-γ-dependent pathway.[21,22] In our study, using a murine model, pulmonary VEGF protein levels were significantly decreased in CS-exposed mice when compared with air-exposed mice. Furthermore, the microarray and histological findings indicate a possible role of AmotL1 in the pathogenesis of emphysema. Amot is a vascular angiogenesis related-protein that can induce endothelial cell migration and tubule formation, thereby promoting angiogenesis. An isoform of AmotL1 functions as a key regulator of endothelial cell migration and cell-cell junction stability.[12] There appeared to be a distinct difference between the vessels that were arrested due to *VEGF*[23] versus *amotL1* knockdown. In *amotl1*

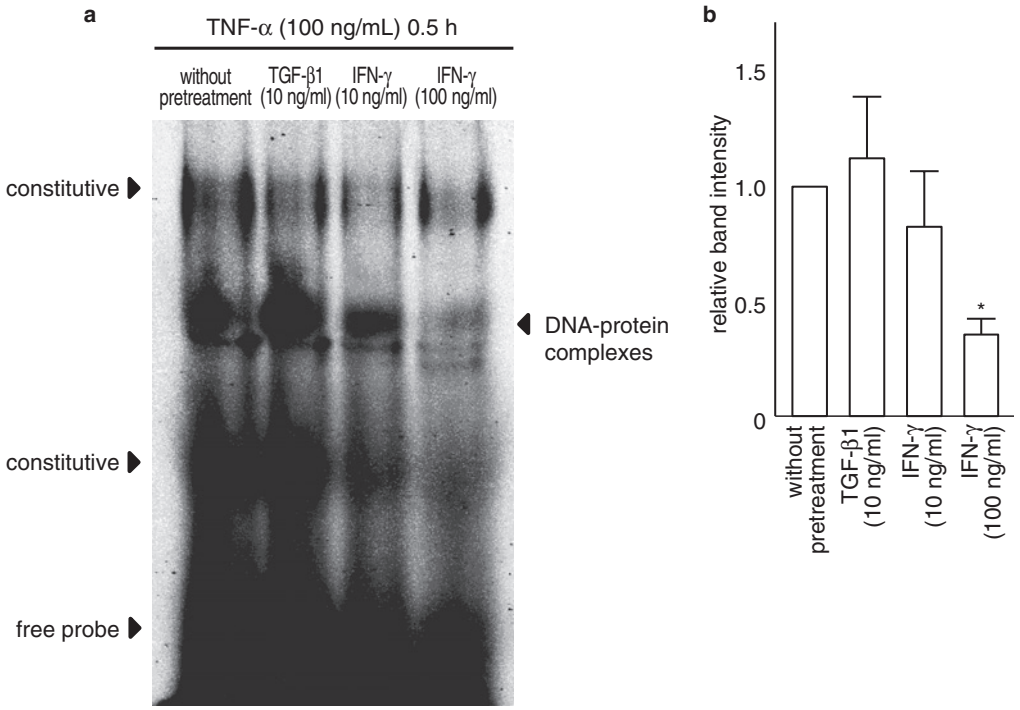

Fig. 6 Effects of IFN-γ on TNF-α-induced AmotL1 DNA binding activity. Electrophoretic mobility shift assay (EMSA) for AmotL1 binding activity. Human lung microvascular endothelial cells (HLMVECs) were pretreated for 72 h with or without TGF-β (10 ng/ml) or IFN-γ (10 ng/ml or 100 ng/ml) and then stimulated with TNF-α (100 ng/ml) for an additional 0.5 h. **a**) The nuclear extracts from cultured HLMVECs were assessed *via* EMSA. **b**) Quantification of the EMSA with the infrared fluorophore-labeled AmotL1 promoter region. Data are the summary (mean ± SE) of five independent experiments. *indicates $p < 0.05$ vs. the no pretreatment condition.

knockdown vessels, sprouting vessels and the spreading of tip cells were arrested, and connections between the stalk cells and the aorta appeared to be destabilized. Consistent with its functions during physiologic angiogenesis in the zebrafish model of blood vessel development, it is tempting to speculate that *amotl1* knockdown mice might have an enlarged airspace of the lungs accompanying the decrease of angiogenic potential. We believe that this response is linked to the cell-cell junction control of the stalk cells, which play striking and distinct roles when compared to down regulated VEGF-induced pathogenesis in developing emphysema.

Based on our present *in vivo* study, we employed *in vitro* cultures of HLMVECs to evaluate the effect of cytokines on AmotL1 expression. IFN-γ levels are lower in the sputa of patients with stable emphysema compared with patients who have exacerbations of emphysema, which is also associated with viral infections.[24] IFN-γ also acts as an anti-angiogenic cytokine and decreases the expression of connective tissue growth factor (CTGF), which induces angiogenesis and regulates endothelial cell function. Moreover, TNF-α interacts in a synergistic fashion with IFN-γ to diminish CTGF expression in lung endothelial cells.[25] Our study demonstrated, unexpectedly, that TNF-α induces the expression of AmtoL1, which is suppressed by IFN-γ. TNF-α is a major inflammatory mediator that induces multiple changes in endothelial cell gene expression, including adhesion molecules, integrins, and matrix metalloproteinases. However, its effects on angiogenesis have been the subject of controversy. Angiogenesis is a multistep process that involves endothelial cell degradation of the adjacent basement membrane, sprouting, proliferation, alignment, tube formation, branching, anastomosis, the synthesis of new basement membranes, the recruitment of parenchymal cells, and a return to quiescence.[26-29] It is possible that TNF-α differentially affects each of these steps. In fact, additional studies have demonstrated that TNF-α primes endothelial cells for angiogenic sprouting by inducing a tip-cell phenotype through NFκB activation.[30,31]

In the present study, EMSAs were performed to determine whether NFκB interacts with the AmotL1 promoter region. To date, it has been demonstrated that there might be multiple transcription-factor-binding sites in the AmotL1 promoter region, but whether they play a critical role in regulating AmotL1 expression in HLMVECs is unknown. All of the

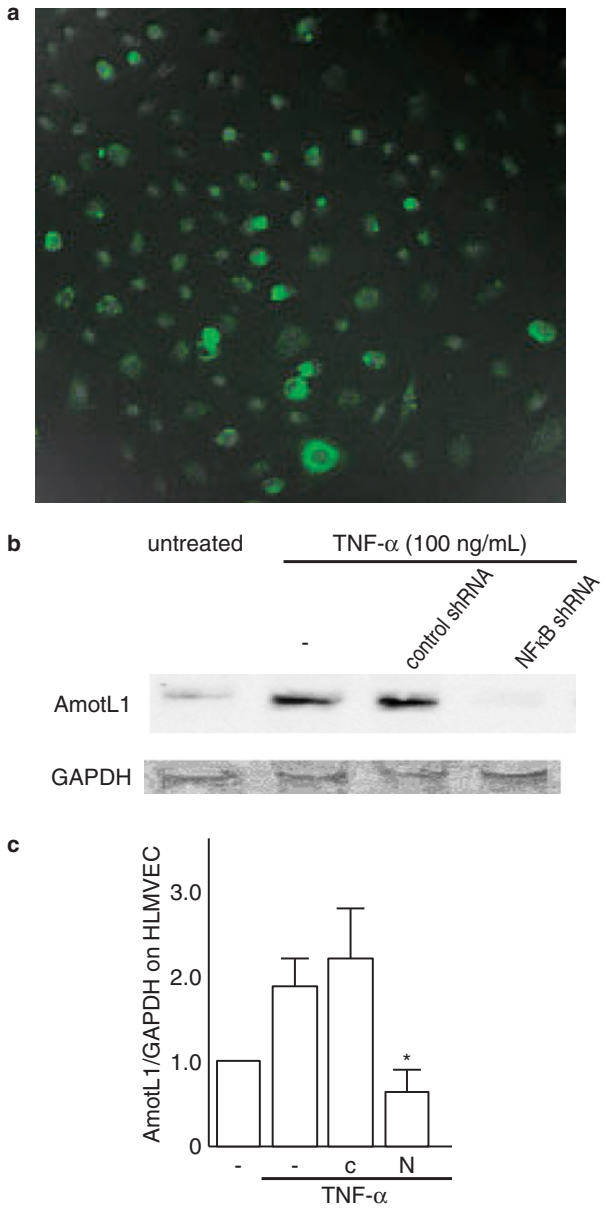

Fig. 7 Generation of stable NFκB-silenced human lung microvascular endothelial cells (HLMVECs) and the effects of NFκB p65 shRNA on TNF-α-induced AmotL1 expression. The selection of stable lines of cell containing the lentiviral-transduced shRNA was accomplished *via* puromycin selection. NFκB is required for TNF-α-induced AmotL1 regulation. **a**) HLMVECs could be effectively transfected with control plasmids. The transfection efficiency was observed by immunofluorescence confocal microscopy. **b**) HLMVECs were pretreated for 16 h with or without shRNA and then stimulated with TNF-α (100 ng/ml) for an additional 24 h. The cellular extracts were immunoblotted for AmotL1 and GAPDH. **c**) The densitometric analysis of AmotL1 production. Data are expressed as the mean ± SE of five independent experiments. *indicates $p < 0.05$ vs. TNF-α stimulation (100 ng/ml) without shRNA. -, without shRNA; C, control shRNA; N, NFκB shRNA.

known AmotL1 sequences were searched for the presence of putative transcription-factor-binding elements using the TRANSFAC database.[19] Based on the data, the GATA-1-binding site (-573/-583), the Stat-5A-binding site (-557/-533) and the NFκB-binding site (-384/-372) contain activating elements. In the present study, we observed that the major promoter region in which NFκB mainly regulates transcription is by binding to the -384 to -372 segment. To confirm the role of NFκB in regulating AmotL1 expression, we transfected HLMVECs with shRNA. Our studies demonstrated that NFκB is necessary for AmotL1 expression in HLMVECs and that IFN-γ interacts at the transcription level with IκBα to reduce AmotL1 expression. Some reports have indicated the ability of IFN-α or IFN-γ to inhibit TNF-α-induced NFκB pathways in various cell types.[32-35] Multiple mechanisms underlying the IFN inhibitory effect on the NFκB pathways have been discussed, including the following mechanisms: 1) preventing IκB degradation[33]; 2) inhibiting the NFκB-DNA interaction[34]; and 3) tightly regulating the TNF-α receptor 1 activity induced by its direct interaction with Stat1 (activated by interferons).[36,37] In our present study, IFN-γ prevented the degradation of IκBα in HLMVECs, and it is conceivable that IFN-γ regulated the TNF-α-induced AmotL1-dependent angiogenesis.

When viewed in combination, our data suggest that TNF-α and IFN-γ are expressed in the airways of mice exposed to CS and that the IFN-γ-mediated-prevention of IκBα degradation contributes to the pathogenesis of pulmonary emphysema, at least in part, *via* its ability to induce the sprouting tip cells of pulmonary structural vessels. It is also likely that the IFN-γ level, which is influenced by viral infections, locally affects signals in the developing vessels. Further examination is necessary to clarify the mechanisms that mediate anti-viral innate immune responses in the pathogenesis caused by decreased AmotL1 levels in the emphysema lung.

The lung tissues from the patients with bronchial asthma and emphysema were all treated with LABA and ICS. Because studies from our laboratory have demonstrated that there were no significant differences in the AmotL1 expression in asthmatic lungs treated with ICS and without ICS (unpublished data), we speculated that this ICS-AmotL1 interaction did not affect the expression of AmotL1 in the lungs. However, it has been reported that both progesterone and estrogen steroids are upregulators of AmotL1 expression.[38] Additional investigation will be required to define the mechanisms of the TNF-α and IFN-γ interaction in the HLMVECs under steroid treatment.

Taken together, our data highlight the importance of AmotL1 in the pathogenesis of emphysema; furthermore, we have identified the precise molecular mechanisms that may assist in furthering our under-

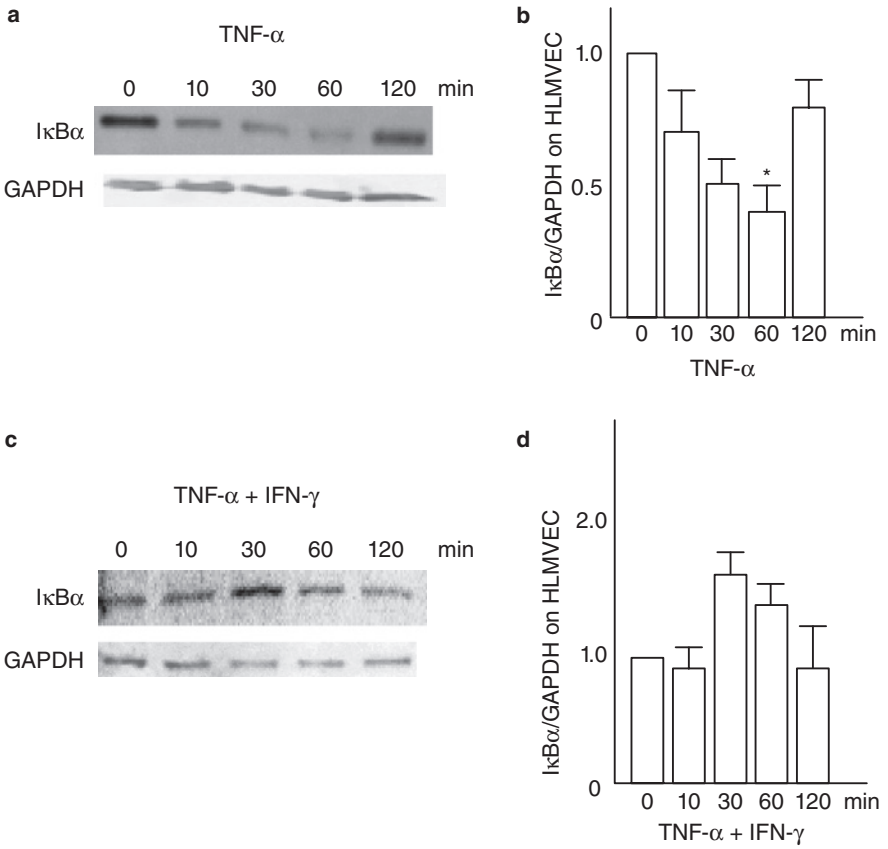

Fig. 8 The effects of IFN-γ on TNF-α-dependent degradation of IκBα. Human lung microvascular endothelial cells (HLMVECs) pretreated with or without 100 ng/ml IFN-γ for 72 h were stimulated with 100 ng/ml TNF-α for the indicated times. The cytosolic fractions were then analyzed by immunoblotting using IκBα and GAPDH antibodies. IFN-γ blocks the TNF-α-induced degradation of IκBα. **a**, **c**) Representative of five separate experiments. **b**, **d**) Summary of the data (mean ± SE) of five independent experiments. *indicates $p < 0.05$ vs. stimulation for 0 min.

standing of the pathology of emphysema.

ACKNOWLEDGEMENTS

The authors would like to acknowledge M. Shibanai and M. Niisato (Iwate Medical University School of Medicine) for their help in performing the study.

REFERENCES

1. Vestbo J, Hurd SS, Agusti AG *et al*. Global Strategy for the Diagnosis, Management and Prevention of Chronic Obstructive Pulmonary Disease, GOLD Executive Summary. *Am J Respir Crit Care Med* 2013;**187**:347-65.
2. Kristan SS, Marc MM, Kern I *et al*. Airway angiogenesis in stable and exacerbated chronic obstructive pulmonary disease. *Scand J Immunol* 2012;**75**:109-14.
3. Moermans C, Heinen V, Nguyen M *et al*. Local and systemic cellular inflammation and cytokine release in chronic obstructive pulmonary disease. *Cytokine* 2011;**56**: 298-304.
4. Di Stefano A, Caramori G, Ricciardolo FL, Capelli A, Adcock IM, Donner CF. Cellular and molecular mechanisms in chronic obstructive pulmonary disease: an overview. *Clin Exp Allergy* 2004;**34**:1156-67.
5. Liebow AA. Pulmonary emphysema with special reference to vascular changes. *Am Rev Respir Dis* 1959;**80**:67-93.
6. Kasahara Y, Tuder RM, Taraseviciene-Stewart L *et al*. Inhibition of VEGF receptors causes lung cell apoptosis and emphysema. *J Clin Invest* 2000;**106**:1311-9.
7. Kasahara Y, Tuder RM, Cool CD, Lynch DA, Flores SC, Voelkel NF. Endothelial cell death and decreased expression of vascular endothelial growth factor and vascular endothelial growth factor receptor 2 in emphysema. *Am J Respir Crit Care Med* 2001;**163**:737-44.
8. Bratt A, Wilson WJ, Troyanovsky B *et al*. Angiomotin belongs to a novel protein family with conserved coiled-coil and PDZ binding domains. *Gene* 2002;**298**:69-77.
9. Ernkvist M, Aase K, Ukomadu C *et al*. p130-angiomotin associates to actin and controls endothelial cell shape. *FEBS J* 2006;**273**:2000-11.
10. Nishimura M, Kakizaki M, Ono Y *et al*. JEAP, a novel component of tight junctions in exocrine cells. *J Biol Chem* 2002;**277**:5583-7.

11. Sugihara-Mizuno Y, Adachi M, Kobayashi Y *et al*. Molecular characterization of angiomotin/JEAP family proteins: interaction with MUPPI/Patj and their endogenous properties. *Genes Cells* 2007;**12**:473-86.

12. Zheng Y, Vertuani S, Nyström S *et al*. Angiomotin-like protein 1 controls endothelial polarity and junction stability during sprouting angiogenesis. *Circ Res* 2009;**105**:260-70.

13. Ramos-Gomez M, Kwak MK, Dolan PM *et al*. Sensitivity to carcinogenesis is increased and chemoprotective efficacy of enzyme inducers is lost in nrf2 transcription factor-deficient mice. *Proc Natal Acad Sci U S A* 2001;**98**:3410-5.

14. Thurlbeck WM. Measurement of pulmonary emphysema. *Am Rev Respir Dis* 1967;**95**:752-64.

15. Saetta M, Shiner RJ, Angus GE *et al*. Destructive index: a measurement of lung parenchymal destruction in smokers. *Am Rev Respir Dis* 1985;**131**:764-9.

16. Nakamura Y, Nagashima H, Akiyama M *et al*. Novel ribbon-type nuclear factor of activated T cells decoy oligodeoxynucleotides preclude airways hyperreactivity and Th2 cytokine expression in experimental asthma. *Int Arch Allergy Immunol* 2011;**155**:129-40.

17. Nagashima H, Nakamura Y, Kanno H, Sawai T, Inoue H, Yamauchi K. Effect of genetic variation of IL-13 on airway remodeling in bronchial asthma. *Allergol Int* 2011;**60**:291-8.

18. Nakamura Y, Esnault S, Maeda T, Kelly EA, Malter JS, Jarjour NN. Ets-1 regulates TNF-alpha-induced matrix metalloproteinase-9 and tenascin expression in primary bronchial fibroblasts. *J Immunol* 2004;**172**:1945-52.

19. Wingender E, Kel AE, Kel OV *et al*. TRANSFAC, TRRD and COMPEL: towards a federated database system on transcriptional regulation. *Nucleic Acids Res* 1997;**25**:265-8.

20. Singh A, Rangasamy T, Thimmulappa RK *et al*. Glutathione peroxidase 2, the major cigarette smoke-inducible isoform of GPX2 in lungs, is regulated by Nrf2. *Am J Respir Cell Mol Biol* 2006;**35**:639-50.

21. Kang MJ, Lee CG, Lee JY *et al*. Cigarette smoke selectively enhances viral PAMP- and virus-induced pulmonary innate immune and remodeling responses in mice. *J Clin Invest* 2008;**118**:2771-84.

22. Ma B, Dela Cruz CS, Hartl D *et al*. RIG-like helicase innate immunity inhibits vascular endothelial growth factor tissue responses via a type I IFN-dependent mechanism. *Am J Respir Crit Care Med* 2011;**183**:1322-35.

23. Jia D, Hasso SM, Chan J *et al*. Transcriptional repression of VEGF by ZNF24: mechanistic studies and vascular consequences in vivo. *Blood* 2013;**121**:707-15.

24. Rohde G, Borg I, Wiethege A *et al*. Inflammatory response in acute viral exacerbations of COPD. *Infection* 2008;**36**:427-33.

25. Laug R, Fehrholz M, Schütze N *et al*. IFN-γ and TNF-α synergize to inhibit CTGF expression in human lung endothelial cells. *PLoS One* 2012;**7**:e45430.

26. Folkman J. Tumor angiogenesis: a possible control point in tumor growth. *Ann Intern Med* 1975;**82**:96-100.

27. Folkman J. Tumor angiogenesis. *Adv Cancer Res* 1985;**43**:175-203.

28. Yancopoulos GD, Davis S, Gale NW, Rudge JS, Wiegand SJ, Holash J. Vascular-specific growth factors and blood vessel formation. *Nature* 2000;**407**:242-8.

29. Conway EM, Collen D, Carmeliet P. Molecular mechanisms of blood vessel growth. *Cardiovasc Res* 2001;**49**:507-21.

30. Sainson RC, Johnston DA, Chu HC *et al*. TNF primes endothelial cells for angiogenic sprouting by inducing a tip cell phenotype. *Blood* 2008;**111**:4997-5007.

31. Johnston DA, Dong B, Hughes CC. TNF induction of jagged-1 in endothelial cells is NFkappaB-dependent. *Gene* 2009;**435**:36-44.

32. Ganster RW, Guo Z, Shao L, Geller DA. Differential effects of TNF-alpha and IFN-gamma on gene transcription mediated by NF-kappaB-Stat1 interactions. *J Interferon Cytokine Res* 2005;**25**:707-19.

33. Manna SK, Mukhopadhyay A, Aggarwal BB. IFN-alpha suppresses activation of nuclear transcription factors NF-kappa B and activator protein 1 and potentiates TNF-induced apoptosis. *J Immunol* 2000;**165**:4927-34.

34. Sancéau J, Boyd DD, Seiki M, Bauvois B. Interferons inhibit tumor necrosis factor-alpha-mediated matrix metalloproteinase-9 activation via interferon regulatory factor-1 binding competition with NF-kappa B. *J Biol Chem* 2002;**277**:35766-75.

35. Keslacy S, Tliba O, Baidouri H, Amrani Y. Inhibition of tumor necrosis factor-alpha-inducible inflammatory genes by interferon-gamma is associated with altered nuclear factor-kappaB transactivation and enhanced histone deacetylase activity. *Mol Pharmacol* 2007;**71**:609-18.

36. Wang Y, Wu TR, Cai S, Welte T, Chin YE. Stat1 as a component of tumor necrosis factor alpha receptor 1-TRADD signaling complex to inhibit NF-kappaB activation. *Mol Cell Biol* 2000;**20**:4505-12.

37. Wesemann DR, Qin H, Kokorina N, Benveniste EN. TRADD interacts with STAT1-alpha and influences interferon-gamma signaling. *Nat Immunol* 2004;**5**:199-207.

38. Matsumoto H, Fukui E, Yoshizawa M, Sato E, Daikoku T. Differential expression of the motin family in the peri-implantation mouse uterus and their hormonal regulation. *J Reprod Dev* 2012;**58**:649-53.